

Visual Chiral Recognition through Enantioselective Metallogel Collapsing: Synthesis, Characterization, and Application of Platinum–Steroid Low-Molecular-Mass Gelators**

Tao Tu,* Weiwei Fang, Xiaoling Bao, Xinbao Li, and Karl Heinz Dötz

A simple protocol to distinguish between left- and right-handed enantiomers is extremely intriguing and useful in pharmacology, biology, and even for daily life.^[1,2] Recently, significant progress in chiral recognition has been achieved based on further development of analytical methodology such as NMR, UV/Vis, CD, and fluorescence spectroscopy.^[3] The straightforward and convenient visual discrimination of enantiomers, however, still remains a major challenge in the design of molecular chiral sensors. Very few examples of visual chiral recognition by discernible changes in color and precipitation have been realized.^[4,5] In particular, the application of molecular gels^[6,7] in visual enantioselective discrimination as highly sensitive nanostructured soft matter susceptible to various stimuli has been widely neglected to date.^[8] Only very recently Pu and co-workers reported a chiral molecular gel prepared from an (*R*)-binol-terpyridine based Cu^{II} complex as a potential visual chiral sensor for the enantiomers of amino alcohols.^[8a]

As one type of the most studied and efficient low-molecular-mass gelators (LMMGs),^[6] aromatic-linker-steroidal (ALS) molecular gels^[6,7] have exhibited potential for application in light and pH sensors.^[6d] To date, however, to our knowledge no report on their potential application in visual enantioselective discrimination is available, although cholesteryl crown ethers have been employed in the chiral recognition of optically active ammonium ions.^[4f] Despite the major role that organometallic compounds play in synthesis, catalysis, and material sciences, there are only very few examples of organometallic compounds that are able to act as

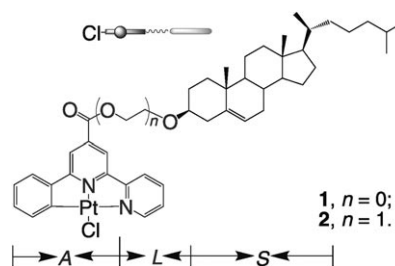
metallogelators,^[9] among them only two organometallic ALS compounds (cholesterol ferrocene^[10] and titanocene derivatives),^[11] which have been developed as efficient LMMGs. Recently, we have developed pyridine-bridged palladium pincer complexes as efficient metallogelators for a variety of organic solvents and ionic liquids in extremely low gelator concentration and demonstrated potential applications in catalysis and solar cells.^[12] π stacking and van der Waals interactions as well as metal–metal bonding are assumed to be responsible for the assembly and aggregation. Following our recent interest in developing novel pincer metallacycles and exploring their potential in soft materials and catalysis,^[12,13] we incorporated a steroidal skeleton to platinum pincer metallacycles to generate a novel type of ALS metallogelators and explored their potential in chiral recognition.

Gelation tests of ALS complexes **1** and **2** (Scheme 1) at a 1 wt% gelator concentration (wt/v; ca. 1.1×10^{-2} M) are summarized in Table 1. Upon heating to reflux in a variety of selected organic solvents and cooling to room temperature, these robust metallogelators entrapped the preferred solvents to form a thermoreversible jelly type of soft material within a few hours, which could be stored under ambient condition without any visible collapse. In contrast to complex **2**, compound **1** turned out to be a less powerful gelator (entries 1–12, Table 1), which may result from the shorter linker of gelator **1** inducing a lower flexibility and lower solubility in most of the solvents applied. ALS metallogelators **1** and **2** efficiently encage polar aprotic solvents such as chloroform, dichloroethane (DCE), dimethylacetamide (DMA), and benzonitrile (PhCN, entries 1–10, Table 1). Complex **2** also immobilized nonpolar aromatic solvents such as benzene and toluene (entries 11, 12, Table 1). The gelation scope of ALS pincer complexes **1** and **2** is further extended by addition of a cosolvent. In the presence of chlorinated solvents, the gelators **1** and **2** also gelate alkanes, alcohols, and acetic acid (see the Supporting Information).

[*] Dr. T. Tu, W. Fang, X. Bao, X. Li
 Shanghai Key Laboratory of Molecular Catalysts and Innovative Materials, Department of Chemistry, Fudan University
 220 Handan Road, 200433, Shanghai (China)
 Fax: (+86) 21-65102412
 E-mail: taotu@fudan.edu.cn
 Prof. K. H. Dötz
 Kekulé-Institute of Organic Chemistry and Biochemistry
 University of Bonn (Germany)

[**] Financial support from the National Natural Science Foundation of China (No. 20902011), the Shanghai Municipal Science and Technology Commission (Qimingxing Program No. 10A1400500), the Shanghai Leading Academic Discipline Project (B108), and Shanghai Key Laboratory of Molecular Catalysts and Innovative Materials (2010MCIMKF04), Department of Chemistry, Fudan University is gratefully acknowledged. We thank Prof. Tao Yi and Prof. Qi-Lin Zhou for technical support.

Supporting information for this article is available on the WWW under <http://dx.doi.org/10.1002/anie.201100620>.



Scheme 1. ALS-type Pt^{II} pincer complexes **1** and **2**.

Table 1: Gelation ability of ALS platinum pincer complexes **1** and **2** in various organic solvents.^[a]

Entry	Solvent	1		2	
		Phase	T_g [°C] ^[b]	Phase	T_g [°C] ^[b]
1	CHCl ₃	G	105	S ^[c]	/
2	CH ₂ Cl ₂	G	/ ^[d]	P ^[c]	/
3	DCE	P ^[c]	/	G	65
4	DMA	G	96	PG	/ ^[d]
5	DMF	I ^[c]	/	G	/ ^[d]
6	DMSO	I ^[c]	/	G	124
7	PhCN	G ^[e]	106	G ^[e]	63
8	dioxane	I ^[c]	/	G	84
9	THF	I ^[c]	/	G	65
10	pyridine	I ^[c]	/	G	/ ^[d]
11	benzene	I ^[c]	/	G	85
12	toluene	I ^[c]	/	G	91

[a] Gelator concentration: 1 wt%; G gel formed at RT, PG partial gel, S solution, P precipitate, I insoluble. [b] Determined by the “dropping ball method”. [c] Gel formed with additional cosolvents (see the Supporting Information). [d] T_g is near RT, hardly detected by the “dropping ball method”. [e] Gel formed with 2 wt% gelator concentration at RT.

The gel–sol phase-transition temperatures (T_g) of the metallogels were determined by the “dropping ball method” (Table 1).^[14] In comparison to its analogue **2**, the gel prepared from the less soluble pincer complex **1** revealed a higher thermostability, as demonstrated by higher T_g values observed for the immobilization of PhCN (106°C vs. 63°C, entry 7, Table 1). Moreover, most gels prepared from mixtures of solvents exhibited higher T_g values than those found for the gels resulting from the corresponding single-component solvents. This observation suggests a practical way to increase the thermal stability of gels. The stability of the gel networks increases with the gelator concentration, as established for the series of **1**/PhCN and **2**/PhCN gels formed with a gelator concentration varying from 1.8–3.2 wt% (Figure S1 in the Supporting Information). Again, the gels obtained from **1** revealed higher T_g values than those resulting from **2**, independent of the applied gelator concentration (see the Supporting Information).

The morphologies of three-dimensional xerogel networks obtained from metallogelators **1** and **2** with the respective solvents were characterized by scanning electron microscopy (SEM). Characteristic images are presented in Figure 1. A 2 wt% gel **1**/PhCN revealed ribbon-like Chinese chives leaves that are approximately 10–50 μm long and up to 3 μm wide (Figure 1a). In contrast, the image of 2 wt% xerogel **2**/PhCN was quite different and revealed very long (up to 20 μm) and thin (ca. 10 nm wide) fibers (Figure 1b). Similar characteristics were found for the gels **1**/DMA and **2**/DMA. The different morphologies between the gels obtained from **1** and **2** suggest that a longer linker between the cholesterol group and the pincer ligand results in a better gelator. Even a low gelator concentration of 1 wt% is sufficient to create a very dense three-dimensional network, as demonstrated by gel **2**/DCE (Figure 1c). Similar xerogel networks were also observed with the gels **2**/dioxane and **2**/benzene (see the Supporting Information). When DCE was used as a cosolvent to assist the gelation of “poorly gelling” solvents (such as

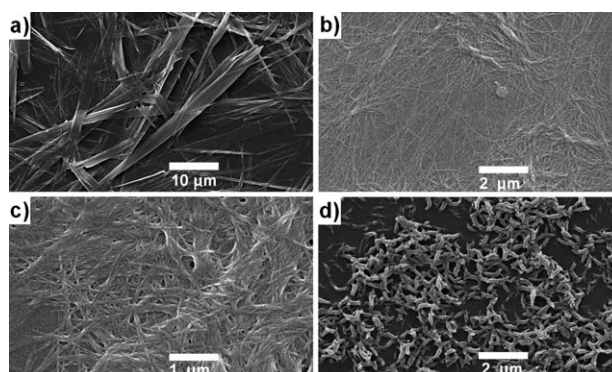
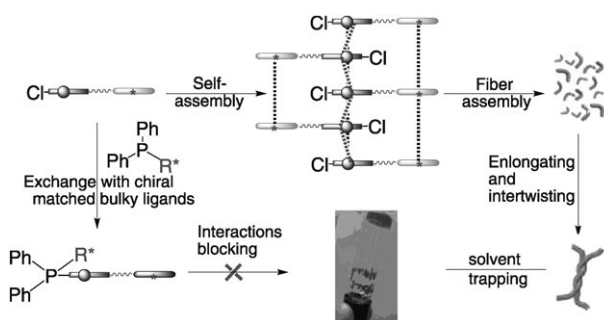


Figure 1. Selected SEM images of gels formed by ALS platinum pincer complexes **1** and **2**: a) Gel **1**/PhCN (2 wt%); b) gel **2**/PhCN (2 wt%); c) gel **2**/DCE (1 wt%); d) gel **2**/(DCE+EtOH) (1 wt%).

EtOH and MeOH), a morphology of short and thick helices was observed (Figure 1d). Similar images were also found with the gels **2**/(CHCl₃+EtOH) and **2**/(CHCl₃+MeOH). Long, thin helical wool-type fibers were encountered with gels prepared from **2** with ACN, EtOAc, hexane, acetone, and HOAc when DCE has been added. These examples clearly demonstrate that the addition of a cosolvent is suited to control the morphologies of xerogels **2**. Gels prepared with metallogelator **1** and a mixture of solvents consisted of long, straight thick fibers. Moreover, straight rods (100–200 nm wide and 3–5 μm long) characterize the morphologies of the gels **2**/DMSO and **2**/DMF (see the Supporting Information).

The various gel network morphologies formed by gelators **1** and **2** inspired us to investigate the principles of the aggregation of the steroid–ligand–metal complex hybrid in the gelation process. Temperature-dependent ¹H NMR spectroscopy studies of gel **2**/[D₆]DMSO (5 wt%) revealed broad signals of low intensity, indicating strong aggregation as characteristic for the gel state at ambient temperature (Figure S38 in the Supporting Information). Upon warming by 10°C steps, the signals of complex **2** steadily sharpened. When the temperature was raised to 95°C, the broad signals still existed, but their intensity had increased, which supports a strong aggregation even at elevated temperature. With increasing temperature the ¹H NMR spectral signals of the steroidal part were shifted upfield (e.g., the signal of the cholesterol-3H was shifted from $\delta = 4.09$ to 3.88 ppm over a temperature window of 70°C), whereas the signals of the heteroaromatic hydrogen atoms were shifted downfield upon heating (e.g. the signal at $\delta = 8.94$ was shifted to 9.00 ppm). These phenomena were thermoreversible and thus reflect both reduced intermolecular van der Waals interactions between the steroidal part and decreasing π – π interactions between coplanar heteroaromatic rings upon warming. These interactions may rationalize the gelator molecular assembly and further coordination of solvents to form solvates within a modified network that is capable of trapping additional solvent, leading to the gel formation (Scheme 2).

To gain further insight into the assembly process, the structure and dimensions of the xerogel networks of **2**/toluene (5 wt%) were studied by X-ray diffraction (Figure S39 in the



Scheme 2. Suggested gel assembly and gel collapsing process through interactions hampered by coordination of bulky phosphine ligands.

Supporting Information).^[15] The major features in the XRD pattern are three broad reflections at $2\theta = 7.8^\circ$ (L_{001}), 15.6° (L_{002}) and 25.6° (d_{001}). L_{001} and L_{002} are assigned to a lamellar structure with a mean distance of 11.38 Å, which may reflect the distance between stacked layers of the gelator molecule. The peak of d_{001} indicates another vital unit with a typical distance of 3.47 Å, which is assumed to result from the corresponding π stacking and metal–metal interactions between the coplanar heteroaromatic rings of the pincer ligands in complex **2**.

Since π stacking and metal–metal interactions are considered as key contributions to the gel formation, structural modifications of the metallogelator suited to hamper these interactions are expected to allow a control over formation and collapse of the gel. According to Che and co-workers, chloride ligands coordinated to platinum or gold pincer complexes readily undergo ligand exchange, for example, by phosphines, alkenes, or other ligands, to give mono-, di- or trinuclear cyclometalated complexes revealing potential in sensor and imaging development.^[16] Therefore, the substitu-

tion of a chloro ligand in complexes **1** and **2** for a bulky phosphine was expected to block the assembly process between the heteroaromatic rings and, thus, to induce a collapse of the gel network owing to the overcrowded ligand sphere (Scheme 2).

Binaphthyl derivatives, such as 2,2'-bis(diphenylphosphino)-1,1'-binaphthyl (binap) and 1,1'-binaphthalene-2,2'-diol (binol), are well-established as powerful ligands in asymmetric transformations^[17] and supramolecular chemistry^[18] owing to their elegant chiral steric hindrance and strong donor properties. Aiming at an unprecedented approach to visual discrimination of enantiomers, we studied the efficiency of metallogelators **1** and **2** in the presence of chiral binap. The addition of one equivalent of (*R*)- or (*S*)-binap to the stable turbid gel **1**/CHCl₃ (1 wt %, Figure 2a) or to gel **2**/toluene with subsequent heating to reflux and cooling to room temperature resulted in a collapse of the metallogels. These results may be rationalized in terms of a substitution of the chloro ligand in complexes **1** and **2** for binap blocking the intermolecular π stacking and metal–metal interactions between the heteroaromatic rings, which finally led to a collapse of the gel network. To determine the minimum amount of chiral binap required for gel collapsing, gradually reduced amounts of (*R*)- or (*S*)-binap were added to samples of gel **1**/CHCl₃. Surprisingly, when the amount of chiral phosphine was reduced to 0.1 equiv (0.36 mg), we observed a striking difference in the behavior of the respective gels: Whereas the gel sample containing (*S*)-binap survived the heating and cooling sequence as a robust gel (Figure 2b), the gel sample containing the (*R*)-binap enantiomer collapsed. Similar phenomena were also observed with other chiral phosphine ligands (see Figures S43 and S44 in the Supporting Information). Further decrease of the amount of chiral phosphine resulted in the conservation of the stable gel network, independent of the binap enantiomer used. This

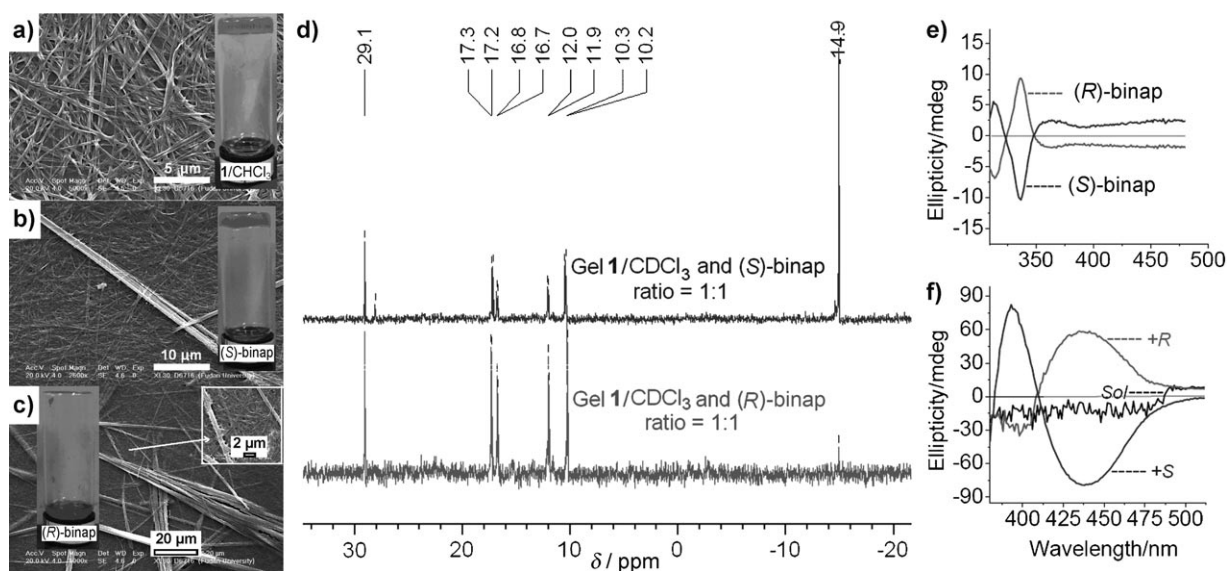


Figure 2. Visual chiral recognition of (*R*)- and (*S*)-binap through ALS platinum gel **1**/CHCl₃ (1 wt%) enantioselective collapsing: SEM images of a) gel **1**/CHCl₃; b) gel (**1** + 0.1 equiv (*S*)-binap)/CHCl₃; c) collapsing sol of (**1** + 0.1 equiv (*R*)-binap)/CHCl₃; d) ³¹P NMR spectra of the solutions prepared with gel **1**/CDCl₃ (1 wt%) and (*S*)-binap or (*R*)-binap; and CD spectra of e) (*R*)- or (*S*)-binap; f) Sol: **1**/CHCl₃ (0.125 wt%); + *R*: Solution prepared with **1**/CHCl₃ (0.125 wt%) and 1 equiv (*R*)-binap; and + *S*: Solution prepared with **1**/CHCl₃ (0.125 wt%) and 1 equiv (*S*)-binap.

exciting phenomenon demonstrates the potential of the metallogel **1**/CHCl₃ in a simple protocol of visual chiral recognition. Further increase or decrease of the amount of (*R*)- and (*S*)-binap added to gel **2**/toluene (0.2 wt %) resulted in a less pronounced differentiation effect: Higher binap concentrations led to the formation of clear orange solutions, while the gel network was preserved when lower binap concentrations were applied, irrespective of the binap enantiomer used.

The influence of the binap additives was further confirmed by an SEM study. In contrast to the SEM morphology of xerogel **1**/CHCl₃ (1 wt %, Figure 2a), the images of (**1** + (*S*)-binap)/CHCl₃ and (**1** + (*R*)-binap)/CHCl₃ reveal additional thick crystalline rods in the fiber networks (Figure 2b,c). In particular, the presence of (*R*)-binap leads to the formation of a dominating agglomerate of crystalline rods (Figure 2c) that are bulkier, denser, and longer than those observed in (**1** + (*S*)-binap)/CHCl₃ (Figure 2b). This difference in superstructure may be responsible for the enantioselective collapse of the gel network. A similar but less pronounced trend of labilization is observed for gel **2**/toluene (0.2 wt %). Thick but less bulky rods which are not suited for an efficient collapse of the gel network are observed in the gel with 0.1 equiv (*R*)-binap (Figure S42 in the Supporting Information). The image of (**2** + (*S*)-binap)/toluene does not reveal any clearly defined crystalline rods, which makes the gel **2**/toluene a less promising candidate for visual chiral recognition. The different gel-collapsing behavior of metallogels obtained from pincer complexes **1** and **2** may be ascribed to the increased molecular flexibility of the extended linker in ALS platinum complex **2**.

A ³¹P NMR spectroscopy study of metallogel **1**/CDCl₃ (1 wt %) in the presence of one equivalent (*R*)- or (*S*)-binap confirmed the chiral recognition results of enantioselective gel collapse and the difference in the SEM morphologies. After one equivalent (*R*)-binap was added to metallogel **1**/CDCl₃ (1 wt %) and the sample was stirred for 48 h at 60 °C to achieve (almost) complete coordination, the signal of (*R*)-binap ($\delta = -14.9$ ppm) had almost vanished; instead, five new intense downfield signals ($\delta = 10.2, 11.9, 16.7, 17.2,$ and 29.1 ppm)—indicative of phosphorus coordination—had appeared (Figure 2d). In an analogous experiment under identical conditions, however, the signal of (*S*)-binap was preserved and turned out to be much more intense than the downfield ³¹P signals. These experiments indicate that the chirality of (*R*)-binap matches the chiral environment of the cholesterol fragment directly attached to the pincer heteroaromatic rings, and the biphosphine readily coordinates to the Pt center in various coordination modes. Further support was provided by high-resolution mass spectrometry (HR-MS) experiments: The substitution of the chloro ligand in complex **1** for (*R*)-binap results in an intense adduct signal of $[M_{(1+binap-C1)} + 1]^+$ (m/z found: 1461.5805; calculated: 1461.5969), whereas its intensity in the analogous experiment applying (*S*)-binap is distinctly weaker (m/z found: 1461.6013, Figures S62 and S63 in the Supporting Information). Accordingly, owing to the hindrance of the bulky binaphthalene skeleton and the PPh₂ group, the π stacking and metal–metal bonding and, thus, the assembly of the metallogelator molecules, are

blocked, leading to the collapse of the gel. Application of (*S*)-binap, however, represents a chiral unmatched case. This enantiomer is difficult to coordinate to the metal center and consequently has no major impact on the assembly process.

The chiral recognition phenomenon of the metallogels established for the binap enantiomers was also characterized by circular dichroism (CD) spectroscopy (Figure 2e,f). Sol **1**/CHCl₃ (0.125 wt %) revealed at room temperature only a weak CD effect between 450 and 500 nm with a split at $[\theta] = 0$ line. In contrast, the orange solution prepared from **1**/CHCl₃ (0.125 wt %) with 1 equiv (*R*)-binap afforded an intensive split CD band crossing the $[\theta] = 0$ line at 415 nm, revealing a slightly negative first and a strong positive second Cotton effect, which significantly differs from the CD pattern observed for (*R*)-binap (Figure 2e). Whereas gelator **1** and (*R*)-binap represent the chiral matched case, the combination of sol **1**/CHCl₃ (0.125 wt %) and (*S*)-binap results in a non-mirror-image CD pattern characterized by a first positive and second negative allosterism.

In conclusion, a method for the visual chiral recognition of (*R*)- and (*S*)-binap has been established through an enantiocontrolled breakdown of gels prepared from novel ALS-type pincer metallogelators **1** and **2**, which may be relevant for the design of chiral sensors. Van der Waals interactions between the steroid part, π stacking of the heteroarene moiety, and metal–metal bonding are responsible for the aggregation. Based on SEM and XRD studies as well as CD and ³¹P NMR spectroscopy, an assembly model has been proposed that is suited to rationalize the potential and scope of these novel ALS pincer platinum metallogels.

Received: January 25, 2011

Revised: March 22, 2011

Keywords: chiral recognition · enantioselectivity · gels · metallacycles · platinum

- [1] a) *Chiral Recognition in the Gas Phase* (Ed.: Z. Anne), Woodhead, Cambridge, UK, **2010**; b) *Chirality in Drug Research* (Eds.: E. Francotte, W. Lindner), Wiley-VCH, Weinheim, **2006**; c) *Chirality in Natural and Applied Science* (Eds.: W. J. Lough, I. W. Wainer), Blackwell, Oxford, UK, **2002**.
- [2] a) Selected recent reviews of chiral recognition: G. A. Hembury, V. V. Borovkov, Y. Inoue, *Chem. Rev.* **2008**, *108*, 1; b) L. Pu, *Chem. Rev.* **2004**, *104*, 1687; c) M. W. Peczu, A. D. Hamilton, *Chem. Rev.* **2000**, *100*, 2479; d) F. Vögtle, P. Knops, *Angew. Chem.* **1991**, *103*, 972; *Angew. Chem. Int. Ed. Engl.* **1991**, *30*, 958.
- [3] a) H.-L. Liu, Q. Peng, Y.-D. Wu, D. Chen, X.-L. Hou, M. Sabat, L. Pu, *Angew. Chem.* **2010**, *122*, 612; *Angew. Chem. Int. Ed.* **2010**, *49*, 602; b) L. Chi, J. Zhao, T. D. James, *J. Org. Chem.* **2008**, *73*, 4684; c) Z.-B. Li, J. Lin, M. Sabat, M. Hyacinth, L. Pu, *J. Org. Chem.* **2007**, *72*, 4905; d) J. Heo, C. A. Mirkin, *Angew. Chem.* **2006**, *118*, 955; *Angew. Chem. Int. Ed.* **2006**, *45*, 941.
- [4] a) S. J. Wezenberg, E. C. Escudero-Adán, J. Benet-Buchholz, A. W. Kleij, *Org. Lett.* **2008**, *10*, 3311; b) B. García-Acosta, R. Martínez-Máñez, J. V. Ros-Lis, F. Sancenón, J. Soto, *Tetrahedron Lett.* **2008**, *49*, 1997; c) W. Kaminsky, E. Haussühl, L. D. Bastin, J. A. Subramony, B. Kahr, *J. Cryst. Growth* **2002**, *234*, 523; d) K. Tsubaki, M. Nuruzzaman, T. Kusumoto, N. Hayashi, B.-G. Wang, K. Fuji, *Org. Lett.* **2001**, *3*, 4071; e) Y. Kubo, S. Maeda, S. Tokita, M. Kubo, *Nature* **1996**, *382*, 522; f) T. Nishi, A. Ikeda, T.

- Matsuda, S. Shinkai, *J. Chem. Soc. Chem. Commun.* **1991**, 339; g) T. Kaneda, K. Hirose, S. Misumi, *J. Am. Chem. Soc.* **1989**, *111*, 742.
- [5] H.-L. Liu, X.-L. Hou, L. Pu, *Angew. Chem.* **2009**, *121*, 388; *Angew. Chem. Int. Ed.* **2009**, *48*, 382.
- [6] Selected recent reviews: a) *Molecular Gels: Materials with Self-Assembled Fibrillar Networks* (Eds.: P. Terech, R. G. Weiss), Springer, Dordrecht, **2006**; b) M. George, R. G. Weiss, *Acc. Chem. Res.* **2006**, *39*, 489; c) "Low Molecular Mass Gelator", *Top. Curr. Chem.* **2005**, 256, 1; d) N. M. Sangeetha, U. Maitra, *Chem. Soc. Rev.* **2005**, *34*, 821; e) F. J. M. Hoeben, P. Jonkheijm, E. W. Meijer, A. P. H. J. Schenning, *Chem. Rev.* **2005**, *105*, 1491; f) L. A. Estroff, A. D. Hamilton, *Chem. Rev.* **2004**, *104*, 1201; g) J. H. van Esch, B. L. Feringa, *Angew. Chem.* **2000**, *112*, 2351; *Angew. Chem. Int. Ed.* **2000**, *39*, 2263.
- [7] a) X. Yu, Q. Liu, J. Wu, M. Zhang, X. Cao, S. Zhang, Q. Wang, L. Chen, T. Yi, *Chem. Eur. J.* **2010**, *16*, 9099; b) J. Wu, T. Yi, T. Shu, M. Yu, Z. Zhou, M. Xu, Y. Zhou, H. Zhang, J. Han, F. Li, C. Huang, *Angew. Chem.* **2008**, *120*, 1079; *Angew. Chem. Int. Ed.* **2008**, *47*, 1063.
- [8] a) X. Chen, Z. Huang, S.-Y. Chen, K. Li, X.-Q. Yu, L. Pu, *J. Am. Chem. Soc.* **2010**, *132*, 7297; b) M. de Loos, J. van Esch, R. M. Kellogg, B. L. Feringa, *Angew. Chem.* **2001**, *113*, 633; *Angew. Chem. Int. Ed.* **2001**, *40*, 613.
- [9] F. Fages, *Angew. Chem.* **2006**, *118*, 1710; *Angew. Chem. Int. Ed.* **2006**, *45*, 1680.
- [10] J. Liu, P. He, J. Yan, X. Fang, J. Peng, K. Liu, Y. Fang, *Adv. Mater.* **2008**, *20*, 2508.
- [11] a) A. Gansäuer, I. Winkler, T. Klawonn, R. J. M. Nolte, M. C. Feiters, H. G. Börner, J. Hentschel, K. H. Dötz, *Organometallics* **2009**, *28*, 1377; b) T. Klawonn, A. Gansäuer, I. Winkler, T. Lauterbach, D. Franke, R. J. M. Nolte, M. C. Feiters, H. Börner, J. Hentschel, K. H. Dötz, *Chem. Commun.* **2007**, 1894.
- [12] a) T. Tu, X. Bao, W. Assenmacher, H. Peterlik, J. Daniels, K. H. Dötz, *Chem. Eur. J.* **2009**, *15*, 1853; b) T. Tu, W. Assenmacher, H. Peterlik, G. Schnakenburg, K. H. Dötz, *Angew. Chem.* **2008**, *120*, 7236; *Angew. Chem. Int. Ed.* **2008**, *47*, 7127; c) T. Tu, W. Assenmacher, H. Peterlik, R. Weisbarth, M. Nieger, K. H. Dötz, *Angew. Chem.* **2007**, *119*, 6486; *Angew. Chem. Int. Ed.* **2007**, *46*, 6368.
- [13] a) T. Tu, X. Feng, Z. Wang, X. Liu, *Dalton Trans.* **2010**, *39*, 10598; b) T. Tu, H. Mao, C. Herbert, M. Xu, K. H. Dötz, *Chem. Commun.* **2010**, *46*, 7796; c) T. Tu, J. Malineni, X. Bao, K. H. Dötz, *Adv. Synth. Catal.* **2009**, *351*, 1029; d) T. Tu, J. Malineni, K. H. Dötz, *Adv. Synth. Catal.* **2008**, *350*, 1791.
- [14] A. Takahashi, M. Sakai, T. Kato, *Polym. J.* **1980**, *12*, 335.
- [15] a) P. Terech, F. Volino, R. Ramasseul, *J. Phys.* **1985**, *46*, 895; b) *Small-Angle X-ray Scattering* (Eds.: O. Glatter, O. Kratky), Academic Press, London, **1982**.
- [16] Selected examples: a) J. J. Yan, A. L.-F. Chow, C.-H. Leung, R. W.-Y. Sun, D.-L. Ma, C.-M. Che, *Chem. Commun.* **2010**, *46*, 3893; b) Y. Chen, K. Li, W. Lu, S. S.-Y. Chui, C.-W. Ma, C.-M. Che, *Angew. Chem.* **2009**, *121*, 10093; *Angew. Chem. Int. Ed.* **2009**, *48*, 9909; c) W. Lu, S. S.-Y. Chui, K.-M. Ng, C.-M. Che, *Angew. Chem.* **2008**, *120*, 4644; *Angew. Chem. Int. Ed.* **2008**, *47*, 4568; d) W. Lu, N. Zhu, C.-M. Che, *Chem. Commun.* **2002**, 900.
- [17] a) J.-H. Xie, Q.-L. Zhou, *Acc. Chem. Res.* **2008**, *41*, 581; b) Y.-M. Li, F.-Y. Kwong, W.-Y. Yu, A. S. C. Chan, *Coord. Chem. Rev.* **2007**, *251*, 2119.
- [18] a) J. Y. Lee, O. K. Farha, J. Roberts, K. A. Scheidt, S. B. T. Nguyen, J. T. Hupp, *Chem. Soc. Rev.* **2009**, *38*, 1450; b) L. Ma, C. Abney, W. Lin, *Chem. Soc. Rev.* **2009**, *38*, 1248.